



High Efficiency Catalytic Transfer Hydrogenation of Furfural to Furfuryl Alcohol Over Metallic Oxide Catalyst

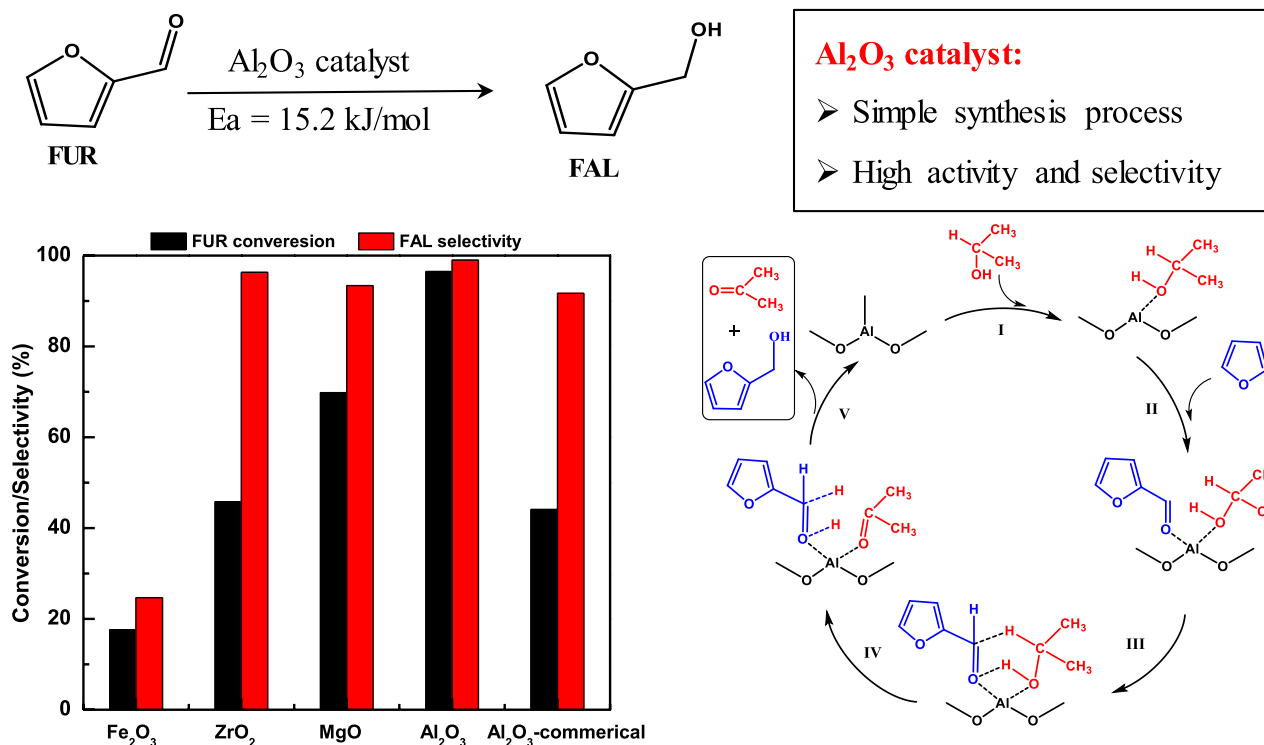
Zonghui Liu¹ · Zhongze Zhang¹ · Zhe Wen¹ · Bing Xue¹

Received: 18 October 2021 / Accepted: 16 January 2022 / Published online: 31 January 2022
© The Author(s), under exclusive licence to Springer Science+Business Media, LLC, part of Springer Nature 2022

Abstract

Development of simple and high performance solid catalysts for the utilization of biomass has become an important research topic in heterogeneous catalysis and sustainable chemistry. Herein, a highly efficient catalytic system was studied for the catalytic transfer hydrogenation of furfural to high value furfuryl alcohol over a series of acidic or basic oxides catalysts. Among those oxides, acidic Al_2O_3 is identified as the most effective for FAL production, giving a FUR conversion as high as 40% (FUR consumption rate was $186 \text{ mmol g}_{\text{cat}}^{-1} \text{ h}^{-1}$) and FAL selectivity of 99% after only 5 min at 150°C using 2-propanol as the H-donor and solvent. Furthermore, the as prepared Al_2O_3 give an E_a value of 15.2 kJ/mol , which is much lower than other complex catalysts in the literatures. Correlating the catalyst performance with its physical and chemical properties uncovers that the large specific surface area and high acidity of Al_2O_3 would be the key to the catalyst performance.

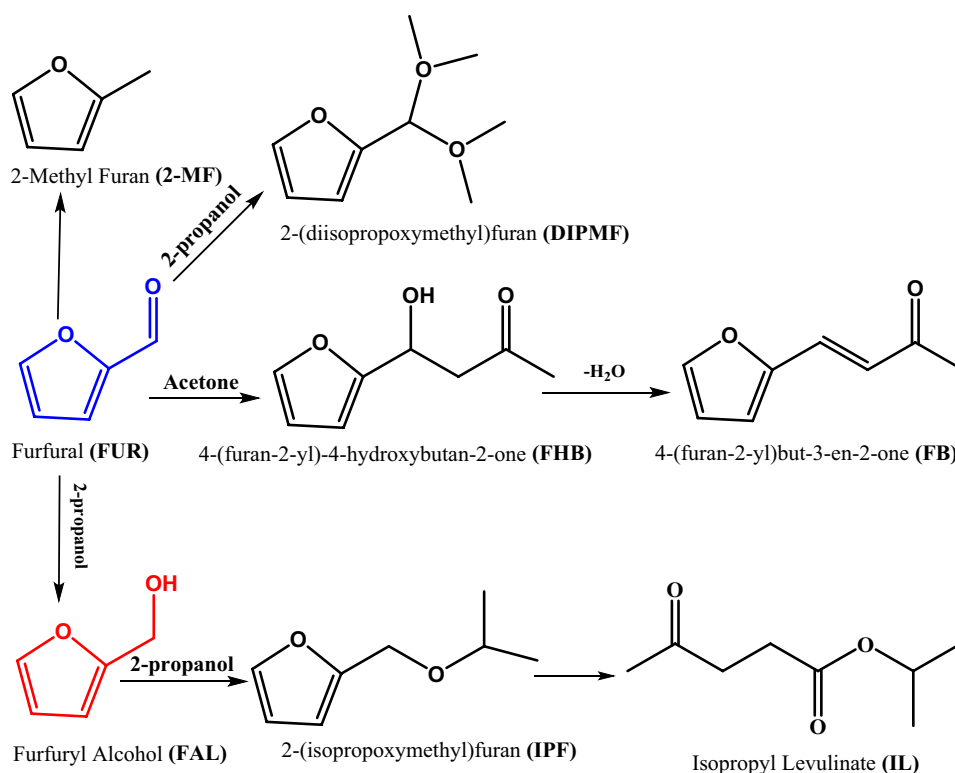
Graphical Abstract



Keywords Furfural · Furfuryl alcohol · Catalytic transfer hydrogenation · Sustainable chemistry

Extended author information available on the last page of the article

Scheme 1 The CTH reaction of FUR and its competing reactions



1 Introduction

At present, with the depletion of fossil resources and the deterioration of the environment, the production of chemicals from biomass has become a hot field [1]. Furfural (FUR), as an important biomass-derived platform, is easily obtained from hemicellulose, and the yearly production of FUR was about 200,000 Tm in the last decade [2, 3]. FUR can convert to many high value chemicals through different reactions, such as hydrogenation [4, 5], oxidation [6–8], oxidation-condensation [9–11], ring opening [12], esterification [13, 14], etc. Among them, around 62% of FUR is estimated to be converted into furfuryl alcohol (FAL) due to its industrial relevance for the manufacture of foundry resins [15]. Commercially, the FAL is produced by the direct hydrogenation over copper-chromite catalysts [16]; however, these catalysts have high toxicity and always produce more environmental problems, some other precious metals (e.g. Pt, Pd, Ir, Ru) [17, 18] was thus used in the direct hydrogenation reaction of FUR. While, the high pressure of H₂ tends to hydrogenate the C=C bonds, resulting in a low selectivity of FAL. On the other hand, the high pressure of H₂ is difficult to store and transport. Therefore, it is necessary to find an economical and efficient process to produce FAL from FUR.

Catalytic transfer hydrogenation (CTH) of α,β -unsaturated aldehydes to the corresponding alcohols using

organic acid or alcohol instead of H₂ as hydrogen donor is a green and sustainable pathway [19]. Because the CTH reaction has the characteristics of non-toxic, high atomic economy, there are many publications dealing with the performance of various catalysts for the CTH reaction of FUR to FAL in recent years. However, this process was always accompanied by several competing reactions and formed 2-Methyl Furan (2-MF), 2-(diisopropoxymethyl) furan (DIPMF), 4-(furan-2-yl)-4-hydroxybutan-2-one (FHB), 4-(furan-2-yl)but-3-en-2-one (FB), 2-(isopropoxymethyl)furan (IPF), and so on, as shown in Scheme 1. FUR is usually produced from the acid catalytic hydrolysis of lignocellulose, which is accompanied by the process with an equal amount of formic acid, which can be used as a hydrogen source for the reduction of FUR [15]. Neeli et al. reported a Rh/ED-KIT-6 as the catalyst and formic acid as the H₂-donor for the CTH reaction of FUR to FAL that gave a 99% selectivity to FAL with 98% conversion of FUR after 5 h at 100 °C [20]. However, the decomposition of formic acid will also produce CO₂, which has a complex effect on the reaction. Not to mention that the acidity of formic acid will corrode the reactor. Alcohol, as a near neutral chemical, overcomes the disadvantages of formic acid as the hydrogen source and becomes an ideal hydrogen donor for CTH reaction. Acid or basic catalysts (e.g., composite metal oxide, zeolites, MOF) are considered to be effective catalysts for the CTH reaction. Very recently, Sancho et al. developed a ZrO₂/Al₂O₃ catalyst for the CTH

of FUR to FAL reaction using 2-propanol as the H-donor and solvent, giving a 95% FUR conversion with a 90% yield of FAL after 5 h at 130 °C [21]. The great number of acid sites and high specific surface area are beneficial to the formation of FAL. Some other complex catalysts were also prepared and used in the CTH of FUR to FAL [20–36], as depicted in Table 1. Strangely, single metal oxide has less been studied in this reaction, although they are widely used in other CTH reactions of other reactants, such as cinnamaldehyde [37, 38], benzenepropanal [39], Levulinic acid [40, 41], cyclohexanone [42–44], crotonaldehyde [45] and so on.

Although composite metal oxides have been widely investigated in the CTH of FUR reaction, reports on FAL production from FUR over single metal oxide are surprisingly less [26, 28, 32, 34]. In this paper, a series of single metal oxides, including acidic (Al_2O_3), basic (MgO), acid–base bifunctional (ZrO_2) and neutral (Fe_2O_3) catalysts were prepared and used to catalyze the CTH of FUR reaction. Several key experimental variables, such as the reaction temperature, the reaction time, the kind of alcohol and the catalyst dosage were optimized to attain the highest FUR conversion and FAL yield. The as-prepared Al_2O_3 catalyst is identified as the most effective for FAL production, giving a FUR conversion as high as 96.5% and FAL selectivity of 99% after 1 h at 150 °C using 2-propanol as the H-donor and solvent, outperforming most catalysts published in the literature. In addition, the FUR to catalyst mass ratio is significantly higher than those employed in the publications (Table 1).

2 Experimental

2.1 Materials

The precursor salts such as, $\text{Al}(\text{NO}_3)_3 \cdot 9\text{H}_2\text{O}$, $\text{ZrOCl}_2 \cdot 8\text{H}_2\text{O}$, $\text{Mg}(\text{NO}_3)_2$, $\text{Fe}(\text{NO}_3)_2$ were supplied by Sinopharm Chemical Reagent Co., Ltd; the precipitant $\text{NH}_3 \cdot \text{H}_2\text{O}$ (25–28%) was obtained by Changzhou Yongfeng Chemical Co. Ltd; furfural (99%), furfuryl alcohol (99%) and solvent (e.g., methanol, ethanol, 1-propanol, 1-butanol, 2-propanol, 2-butanol) were purged from Aladdin. All chemicals were directly used in the experiments without further purification.

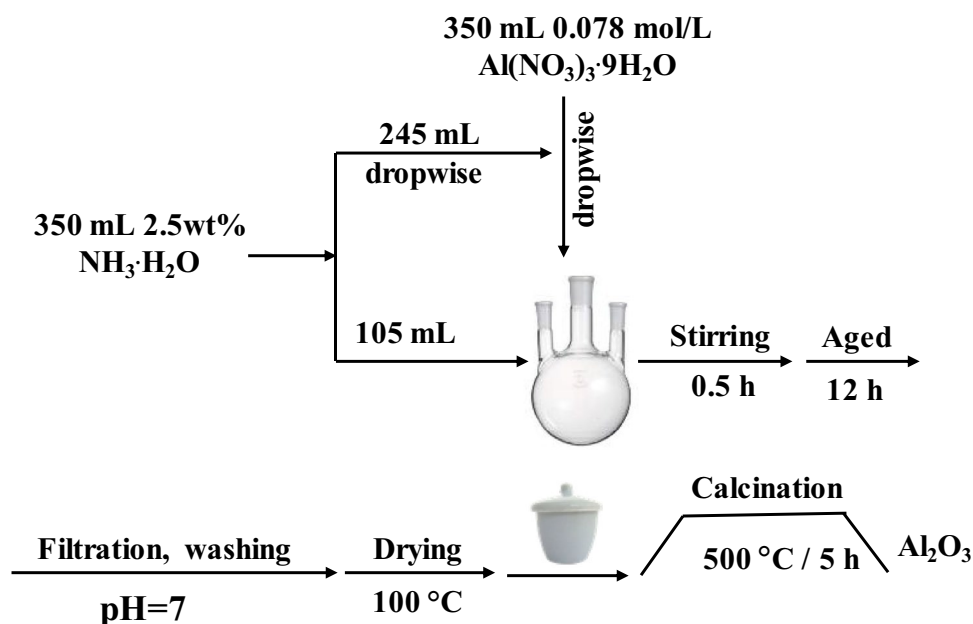
2.2 Catalyst Preparation

All the metal oxides were prepared by precipitation method. For Al_2O_3 (Scheme 2), 105 mL of an aqueous solution of 2.5 wt% $\text{NH}_3 \cdot \text{H}_2\text{O}$ were added in the three-neck flask. 350 mL of an aqueous solution of 0.078 M $\text{Al}_2(\text{NO}_3)_3$ and 245 mL 2.5 wt% $\text{NH}_3 \cdot \text{H}_2\text{O}$ were added dropwise into the three-neck flask under strong stirring. $\text{Al}_2(\text{NO}_3)_3$ and $\text{NH}_3 \cdot \text{H}_2\text{O}$ were completed simultaneously by adjusting the flow rate. After the process finished, the mixture solution was continued stirring for 0.5 h, then aged for 12 h at room temperature before the product precipitates were collected by filtration. The precipitate was then washed with deionized water until neutral. Finally, the solid powers were dried overnight at 110 °C and calcined at 500 °C for 5 h in a muffle furnace.

Table 1 Comparison of the catalytic performance of the as-prepared Al_2O_3 and other reported catalysts to the CTH of FUR to FAL using 2-propanol as H-donor

Catalyst	FUR/Catalyst (mass ratio)	Temp. (°C)	Time (h)	Conv. (%)	Sel. (%)	Yield (%)	Reference
Rh/ED-KIT-6	–	100	4	98	99	97	[20]
$\text{ZrO}_2/\text{Al}_2\text{O}_3$	1	130	5	95	95	90	[21]
$\text{Pd}/\text{Fe}_2\text{O}_3$	0.077	150	7.5	66	96	81	[22]
$\text{Ni-Cu}/\text{Al}_2\text{O}_3$	–	200	4	95	99	94	[23]
Fe-L1/C-800	1	160	15	92	83	76	[24]
ZrPN	2.4	140	2	98	99	98	[25]
Nano-NiO	2.4	150	4	85	96	81	[26]
$\text{Al}_7\text{Zr}_3@/\text{Fe}_3\text{O}_4$	4.8	180	4	99	92	91	[27]
20%Cu/MgO- Al_2O_3	4	210	1	98	90	88	[28]
La FeO_3 -NA	0.8	180	3	90	94	84	[29]
Zr-PW	0.48	120	1	99	99	98	[30]
BZC	0.64	80	5	98	99	97	[31]
Fe_3O_4 -12	0.64	160	5	98	92	90	[32]
ZrPO_4	1.9	120	6	95	76	72	[33]
Co_3O_4 - Al_2O_3	2.3	150	6	76	97	74	[34]
$\text{Fe}_3\text{O}_4@/\text{C}$	3.8	200	4	94	99	93	[35]
UiO-66	3.8	180	1	99	88	87	[36]
Al_2O_3	3.8	150	1	94	99	93	This work

Scheme 2 Preparation route of Al_2O_3 catalyst



ZrO_2 , MgO and Fe_2O_3 catalysts were synthesized by the same process as Al_2O_3 , and their precursors were $\text{ZrOCl}_2 \cdot 8\text{H}_2\text{O}$, $\text{Mg}(\text{NO}_3)_2$ and $\text{Fe}(\text{NO}_3)_3$, respectively.

2.3 Catalyst Characterization

X-ray diffraction (XRD) patterns of the catalysts were measured on a D/max 2500 PC X-ray diffractometer (Rigaku) with a graphite monochromator using Ni-filtered $\text{Cu-K}\alpha$ ($\lambda = 0.15406 \text{ nm}$) radiation at 40 kV and 40 mA. The patterns were recorded over $2\theta = 10\text{--}70^\circ$ at a rate of $10^\circ/\text{min}$. The surface area, pore volume and pore diameter data were obtained by N_2 adsorption–desorption (ASAP 2020 instrument) at 77 K. The specific surface areas were calculated based on the Brunauer–Emmet–Teller method, and pore size distributions were determined by the Barret–Joyner–Halenda method. The acid properties of the samples were evaluated by NH_3 -TPD using ChemBET-3000. The samples (0.2 g) were first pretreated under He atmosphere (80 mL min^{-1}) at $500 \text{ }^\circ\text{C}$ for 1 h and then cooled to $100 \text{ }^\circ\text{C}$ for adsorption of NH_3/He (30 min). After purging with Ar to remove the reversibly adsorbed NH_3 , the sample was finally heated from $100 \text{ }^\circ\text{C}$ to $500 \text{ }^\circ\text{C}$ at a rate of $10 \text{ }^\circ\text{C min}^{-1}$ in flowing Ar.

2.4 Catalytic Reaction

The catalytic transfer hydrogenation reaction of FUR with alcohol was conducted in a stainless steel autoclave (25 mL). A typical procedure for the reaction is described as follows: 50 mg of catalyst, 2 mmol of FUR, 10 mL of alcohol were added into the autoclave. The autoclave is sealed and purged with N_2 (0.8 MPa) 3 times to replace the air, finally, 0.8 MPa N_2 was introduced to the autoclave. The reactor was heated

to reaction temperature under stirring. After the reaction, the autoclave was cooled immediately using ice water, and the reaction products were analyzed by GC (SP-7860) with a FFAP capillary column and a flame ionization detector (FID). Conversion of FUR and selectivity of FAL were calculated according to the following calculations:

$$\text{FUR conversion}(\%) = \frac{\text{moles of FUR reacted}}{\text{moles of FUR in the feed}} \times 100\%$$

$$\text{FAL selectivity}(\%) = \frac{\text{moles of FAL in the product}}{\text{moles of FUR reacted}} \times 100\%$$

The catalytic activity was expressed as mass-specific rates according to the consumption of FUR and formation rate of FAL, which were obtained using the following equation:

$$\begin{aligned} \text{FUR consumption rate} \\ = \frac{\text{moles of FUR consumed per hour (mol/h)}}{\text{weight of catalyst (g)}} \end{aligned}$$

$$\text{FAL formation rate} = \frac{\text{moles of FAL formed per hour (mol/h)}}{\text{weight of catalyst (g)}}$$

3 Results and Discussion

3.1 Catalyst Characterization

Figure 1 shows the XRD patterns of prepared metal oxide catalyst. All samples showed their corresponding diffraction

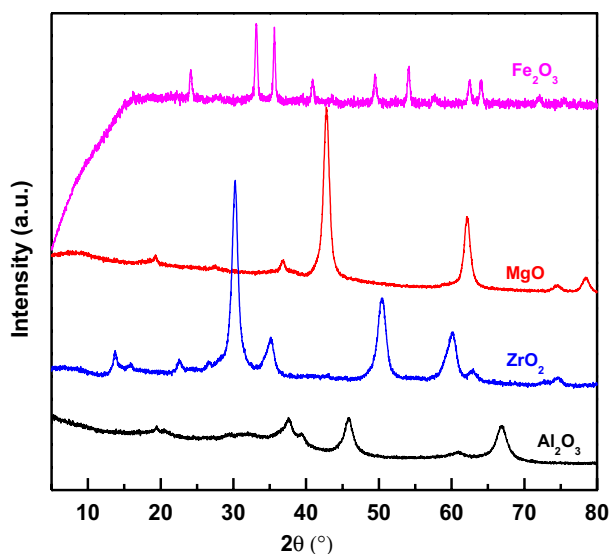


Fig. 1 XRD spectra of metal oxide catalyst

peaks. No impurity peaks appeared in those XRD patterns, indicating that the purity of all those catalysts is very high.

The texture properties of catalysts were analyzed by N_2 physical adsorption–desorption isotherms at 77 K. The curves of adsorption–desorption isotherms and pore size distributions are shown in Fig. 2. All samples showed the Type IV isotherms, indicating the existence of mesoporous structure in all catalysts (Fig. 2A). Both prepared and commercial Al_2O_3 samples showed a long and narrow H_3 type hysteresis loop at a wide relative pressure ($P/P_0 = 0.42 \sim 0.95$), indicating that Al_2O_3 has a typical mesoporous feature, which agrees well with the literature [38]. ZrO_2 presented a H_2 type hysteresis loop at $P/P_0 = 0.65 \sim 0.88$, MgO and Fe_2O_3 exhibited an H_1 type hysteresis loop at a relatively narrow

$P/P_0 = 0.90 \sim 0.98$. In addition, the pore size distribution of Al_2O_3 and ZrO_2 is relatively narrow compared to MgO and Fe_2O_3 samples (Fig. 2B). The detailed textural properties (surface area, pore volume and pore diameter) of samples were summarized in Table 2. The prepared Al_2O_3 had the largest BET surface area of $295 \text{ m}^2 \text{ g}^{-1}$, as well as the highest total volume ($0.36 \text{ cm}^3 \text{ g}^{-1}$) and lowest pore diameter (3.7 nm), which is also in line with the TEM result (Fig. S1). The commercial Al_2O_3 had a lower surface area ($131 \text{ m}^2 \text{ g}^{-1}$) and pore volume ($0.22 \text{ cm}^3 \text{ g}^{-1}$) than the as prepared Al_2O_3 . Fe_2O_3 showed the lowest surface area ($29 \text{ m}^2 \text{ g}^{-1}$) and pore volume ($0.05 \text{ cm}^3 \text{ g}^{-1}$).

NH_3 -TPD and CO_2 -TPD were measured to study the acid–base properties of the prepared catalysts. Because the calcination temperature of those samples was $500 \text{ }^\circ\text{C}$, the highest temperature of NH_3 or CO_2 desorption was thus set at $500 \text{ }^\circ\text{C}$. As seen in Fig. 3A, the Al_2O_3 and ZrO_2 samples had significantly broad peaks of NH_3 desorption from about $180 \text{ }^\circ\text{C}$ to $500 \text{ }^\circ\text{C}$. The peak temperature of Al_2O_3 ($250 \text{ }^\circ\text{C}$) is

Table 2 The textural and acidity–basicity properties of the catalysts

Catalyst	Surface area ($\text{m}^2 \text{ g}^{-1}$)	Pore volume ($\text{cm}^3 \text{ g}^{-1}$)	Pore diameter (nm)	Acidity ^b ($\mu\text{mol g}^{-1}$)	Basicity ^b ($\mu\text{mol g}^{-1}$)
Al_2O_3	295	0.36	3.7	153.9	33
$Al_2O_3^a$	131	0.22	4.7	77.6	29
ZrO_2	114	0.29	7.2	83.6	19
Fe_2O_3	29	0.05	5.6	3.1	0
MgO	34	0.22	11.2	9.9	201

^a Al_2O_3 was obtained by company; ^bThe acidity and basicity were measured according to the NH_3 - and CO_2 -TPD, respectively

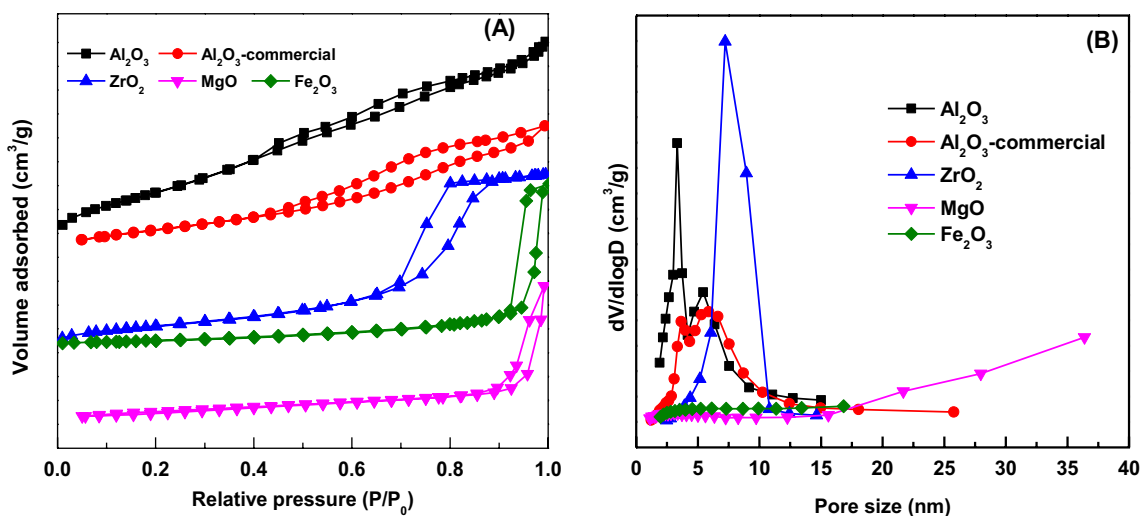


Fig. 2 N_2 adsorption–desorption isotherms (A) and the pore size distributions (B) of the prepared catalyst

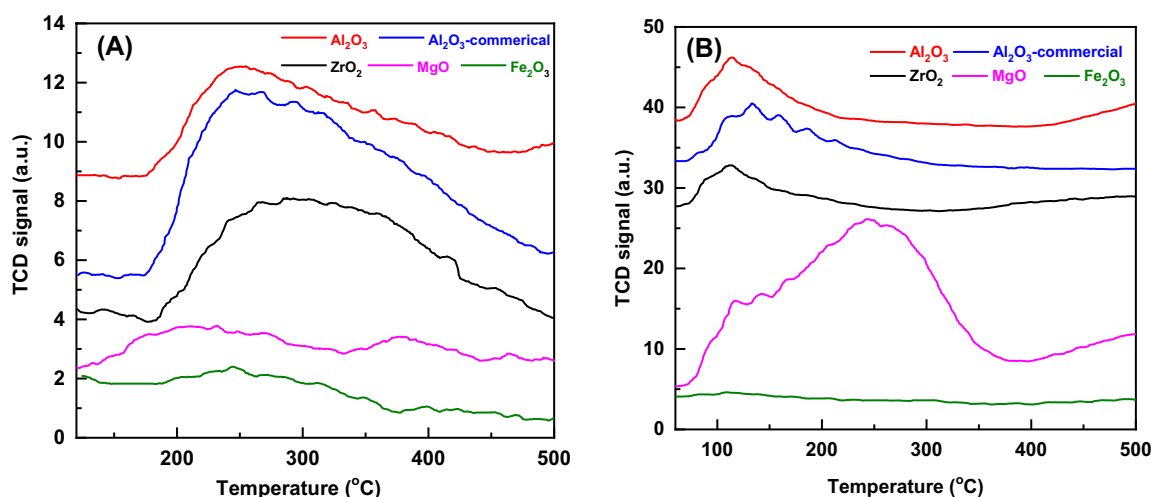


Fig. 3 A NH_3 -TPD and B CO_2 -TPD of metal oxide catalyst

lower than that of ZrO_2 (300 °C), suggesting that both Al_2O_3 and ZrO_2 have weak acid sites and the acid strength of Al_2O_3 is slightly lower than that of ZrO_2 . In addition, the prepared Al_2O_3 has higher acidity than commercial Al_2O_3 . Maybe this is why the prepared Al_2O_3 has better catalytic performance than commercial Al_2O_3 . While, Fe_2O_3 has almost no obvious peak of NH_3 desorption, indicating that there are a few acid sites in Fe_2O_3 sample. In addition, small NH_3 desorption peaks also appeared in the MgO sample, which is consistent with literature reports [26]. Landau et al. also determined the surface acidity of MgO by the n-butylamine titration method [46]. The base properties of catalysts were shown in Fig. 3B, the CO_2 desorption temperature of Al_2O_3 and ZrO_2 were similar and relative low (110 °C), indicating the weak basic sites existed on the surface of catalysts. As was expected that the MgO sample showed a strong base strength (peak temperature at 250 °C) and medium basic sites. The density of the surface acidic and basic sites was also calculated and listed in Table 2. The prepared Al_2O_3 showed the highest acidity ($153.9 \mu\text{mol g}^{-1}$), flowed by ZrO_2 ($83.6 \mu\text{mol g}^{-1}$) and commercial Al_2O_3 ($77.6 \mu\text{mol g}^{-1}$). Fe_2O_3 and MgO

contained few acid sites, which were 3.1 and $9.9 \mu\text{mol g}^{-1}$ respectively. Expectedly, MgO as an alkaline oxide exhibited large numbers of basic sites ($201 \mu\text{mol g}^{-1}$). Al_2O_3 and ZrO_2 has few basic sites, and there are almost no basic sites on Fe_2O_3 surface. Those results are consistent with the data in the literature [26, 27, 39].

3.2 Catalytic Performance

3.2.1 Catalyst Screening

The CTH reaction of FUR with 2-propanol was carried out at 150 °C for 1 h over different metal oxide catalysts and the results were shown in Table 3. It is seen that, except Fe_2O_3 catalyst, the main product was FAL (selectivity: 91.7~99.0%). A number of very minor byproducts were also detected and confirmed by GC-MS analysis (as shown in Scheme 1), including DIPMF (acetalization reaction between FUR and 2-propanol), 2-MF (excessive hydrogenation of FUR), FHB (reaction of FUR with acetone), FB (dehydration of FHB), IPF (etherification of FAL with

Table 3 Catalyst screening for the CTH of FUR^a

Entry	Catalyst	FUR conversion (%)	FAL selectivity (%)	FAL yield (%)	FAL formation rate ($\text{mmol g}_{\text{cat}}^{-1} \text{h}^{-1}$)
1	Blank	1.9	—	—	0.2
2	Fe_2O_3	17.6	24.7	4.3	1.7
3	ZrO_2	45.8	96.3	44.1	17.6
4	MgO	69.8	93.4	65.2	26.1
5	Al_2O_3	96.5	99.0	95.5	38.6
6	$\text{Al}_2\text{O}_3^{\text{b}}$	44.1	91.7	40.4	16.9

^a Reaction conditions: 2 mmol FUR, 10 mL 2-propanol, 50 mg catalyst, 0.8 MPa N_2 , T = 150 °C, t = 1 h.

^b Al_2O_3 was obtained by the company

2-propanol) [27, 33, 47, 48]. The selectivity for those minor products was less than 2%, thus we did not list them in Table 3. As expected, no FAL was detected in the absence of catalyst, indicating that the noncatalyzed process could not occur in the CTH reaction of FUR and 2-propanol (Entry 1). Using Fe_2O_3 as the catalyst, only 17.6% conversion of FUR with 24.7% selectivity of FAL were obtained (Entry 2), meanwhile, about 60% selectivity of acetalization product (DIPMF) was formed by the acid site of the catalyst surface. ZrO_2 as an acid–base catalyst offered a 45.8% FUR conversion and 96.3% FAL selectivity (Entry 3), Zr-based catalysts were also effective for the CTH reaction with other reactants in the reference [21, 27, 33, 49]. In addition, a 69.8% conversion and 93.4% selectivity were obtained over the base MgO catalyst (Entry 4), MgO was also found to be active for other CTH reactions [39, 50]. Very interesting, the highest FUR conversion (96.5%) and FAL selectivity (99.9%) were achieved with the acid Al_2O_3 catalyst (Entry 5), and showed the highest FAL yield (96.4%) and FAL formation

rate ($38.6 \text{ mmol g}_{\text{cat}}^{-1} \text{ h}^{-1}$). The GC image was shown in Fig. S2. For comparison, the commercial Al_2O_3 was used in this reaction, only 44.1% FUR conversion was obtained (Entry 6), which is agreed with the same reaction in the reference [51]. It indicated that the as prepared Al_2O_3 can effectively catalyze FUR to FAL compared to other metal oxide catalysts. It has been known that acidity sites play an important role in the CTH reaction when using alcohol as H-donor [21, 26, 37, 48, 52]. An attempt is made to correlate the FAL yield with the surface acidity and surface area of the catalysts (except for MgO) and the results were shown in Fig. 4. It is clear that the FAL yield increased with increasing the surface acidity and surface area. The Fe_2O_3 with near neutral and lowest surface area presented the lowest FAL yield (4.3%), and Al_2O_3 with the largest surface area and the highest density of surface acidic showed the highest FAL yield (95.5%). It should be mentioned that the basic MgO also gave a relatively high FAL yield (65.2%), which agrees with many earlier reports [39, 50].

3.2.2 Effect of H-Donor

To reveal the influence of H-donor on the performance of Al_2O_3 catalyst, several alcohols include C1 to C4 alcohols, primary and secondary alcohols were chosen and used in the CTH of FUR to FAL reaction. It shows in Table 4 that all of the alcohols could offer the hydrogen atom for FUR. When primary alcohols (methanol, ethanol, 1-propanol and 1-butanol) were used as H-donor (Entry 1–4), the FUR conversion (28.5 ~ 48.5%) and FAL yield (1.3 ~ 39.4%) were much lower than that of secondary alcohol (2-propanol and 2-butanol). This is because secondary alcohols have a lower reduction potential than primary alcohols [38, 52]. The acetalization was the main reaction in methanol and thus showed the lowest FAL selectivity (2.6%) [32, 53]. 1-propanol and 2-propanol showed the higher FUR conversion (40.8% and 96.5%) than that of 1-butanol and 2-butanol (28.5% and 75%), respectively, which is due to the steric effect caused by the longer carbon chain of 2-butanol [53]. Combined with the FUR conversion and FAL selectivity, 2-propanol was the most effective H-donor and reaction

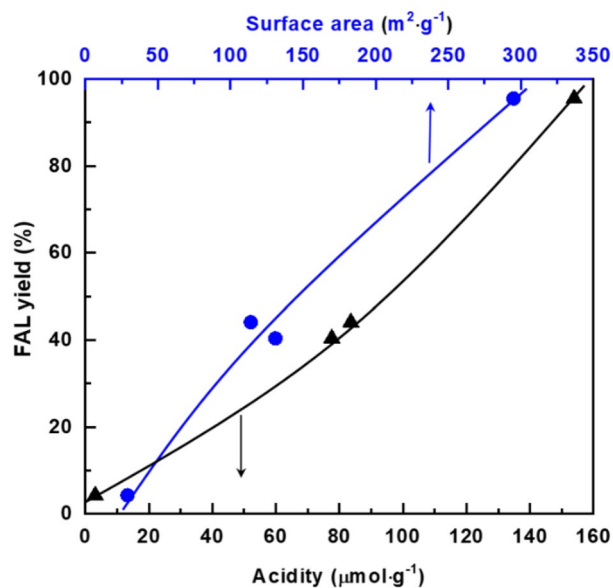


Fig. 4 Dependence of the FAL yield to total acidity (Black filled triangle) and specific surface area (Blue filled circle)

Table 4 The influence of alcohols in the CTH of FUR over Al_2O_3 catalyst^a

Entry	H-donor	FUR conversion (%)	FAL selectivity (%)	FAL yield (%)	FAL formation rate ($\text{mmol g}_{\text{cat}}^{-1} \text{ h}^{-1}$)
1	Methanol	48.5	2.6	1.3	0.5
2	Ethanol	42.8	84.4	36.1	14.4
3	1-propanol	40.8	94.1	39.4	15.3
4	1-butanol	28.5	87.8	25.0	10.1
5	2-propanol	96.5	99.0	95.5	38.6
6	2-butanol	75.0	99.2	74.4	29.8

^aReaction conditions: 2 mmol FUR, 10 mL 2-propanol, 50 mg Al_2O_3 , 0.8 MPa N_2 , $T = 150 \text{ }^\circ\text{C}$, $t = 1 \text{ h}$

solvent for the CTH reaction of FUR to FAL. Those results agree well with earlier literature over other catalysts [26, 30, 32, 53].

3.2.3 Effect of Temperature and Time

The effect of the reaction temperature in the range of 110–150 °C and reaction time in the range of 5–60 min on the catalytic performance of Al_2O_3 catalyst were investigated using 2-propanol as the H-donor, the results are shown in Fig. 5. The reaction temperature and time had little effect on the selectivity of FAL but had a big influence on FUR conversion. The effect of temperature on FUR conversion and FAL selectivity at 60 min are shown in Fig. 5A. The FAL selectivity was higher than 95% regardless of temperature, and the FUR conversion increased from 42% to 96% when temperature increased from 110 °C to 150 °C. By measuring the effect of temperature on FUR consumption rates could obtain the apparent activation energy (E_a) over Al_2O_3 catalyst. The Arrhenius plots were shown in Fig. S3, and the value of E_a is 15.2 kJ/mol. Which is much lower than the results of other catalysts [26, 27, 31, 36, 47, 49, 54, 55]. The effect of reaction time on FUR conversion and FAL selectivity at 150 °C are shown in Fig. 5B. To our surprise, the FUR conversion reached almost 40% in just 5 min of the reaction. The consumption rate was as high as $186 \text{ mmol g}_{\text{cat}}^{-1} \text{ h}^{-1}$. The FUR conversion increased to 96% with increasing the reaction time to 60 min. The FAL selectivity was always higher than 95%. Hence, the FAL yield could reach as higher as 96% for only one hour at 150 °C, and the catalytic

performance of this catalyst was much higher than that of the most catalysts published in literatures, as listed in Table 1.

3.2.4 Effect of Catalyst Dosage

The effect of catalyst dosage on the catalytic performance of FUR to FAL was also studied at 150 °C and 1 h using 2-propanol as the H-donor. It can be seen from Fig. 6 that the selectivity of FAL was always higher than 90% regardless

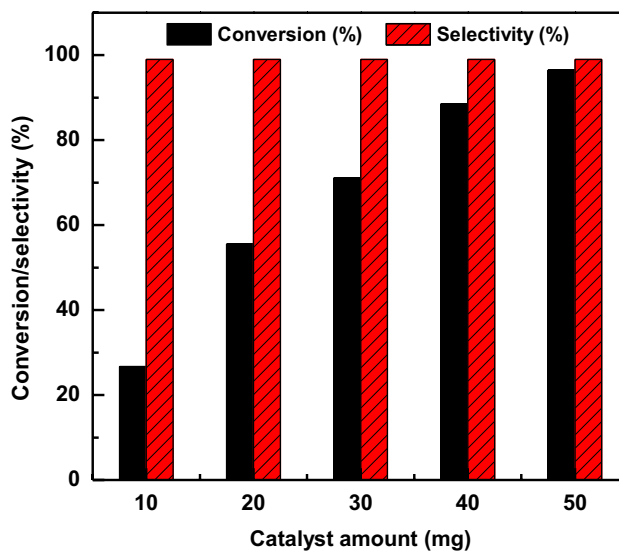
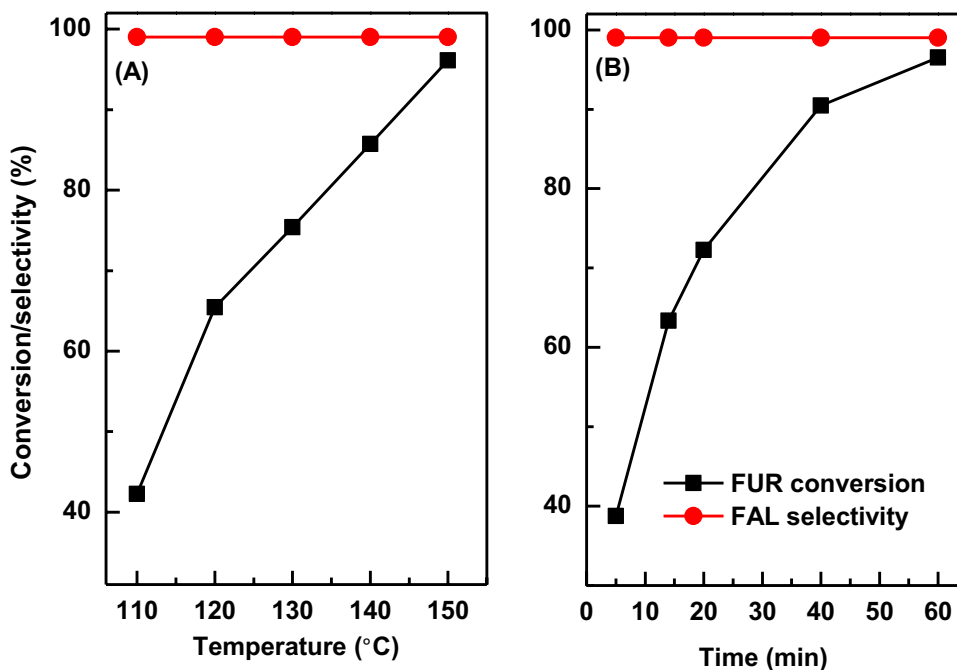


Fig. 6 The effect of the amount of Al_2O_3 on the CTH reaction of FUR to FAL. Reaction conditions: 2 mmol FUR, 10 mL 2-propanol, 0.8 MPa N_2 , $T = 150 \text{ }^\circ\text{C}$, $t = 1 \text{ h}$

Fig. 5 Effect of reaction temperature (A) and reaction time (B) on the catalytic performance of Al_2O_3 for the CTH reaction of FUR to FAL. Reaction conditions: 2 mmol FUR, 10 mL 2-propanol, 50 mg Al_2O_3 , 0.8 MPa



of the catalyst amount. The FUR conversion increased more than two times (from 26% to 56%) with increasing the catalyst dosage from 10 mg to 20 mg. Further increased the amount of Al_2O_3 to 50 mg, the conversion of FUR increased to 96% slowly. Therefore, the preferred Al_2O_3 amount was 50 mg in the CTH reaction of FUR to FAL.

3.2.5 CTH Reaction of Various Aldehydes

The CTH reaction of other aldehydes to the corresponding alcohols over as prepared Al_2O_3 catalyst using 2-propanol as the H-donor and solvent at 150 °C was also performed. As shown in Table 5, the prepared Al_2O_3 showed high activity of aldehydes and selectivity to the corresponding alcohols, especially to benzaldehyde (Entry 1), 66% conversion and 99% selectivity for benzyl alcohol after 1 h. For the derivatives of benzaldehyde (e.g., 4-nitrobenzaldehyde, p-methyl benzaldehyde, p-fluorobenzaldehyde), due to the steric hindrance, a longer reaction time or higher reaction temperature was needed to obtain the higher activity of Al_2O_3 catalyst (Entry 2–4). In addition, a 58% conversion of salicylaldehyde and 72% selectivity of 1,2-phenylenedimethanol were obtained (Entry 5). Moreover, Al_2O_3 can also catalyze the aliphatic aldehydes to the corresponding alcohols (Entry 6). Therefore, the prepared Al_2O_3 also showed a good catalytic performance for the other aldehydes. In combination with the simple preparation and low cost, the Al_2O_3 catalyst has a good industrial application.

3.3 Possible Reaction Mechanism

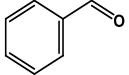
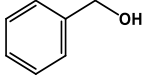
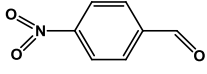
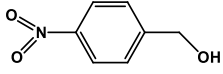
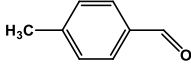
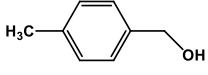
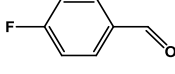
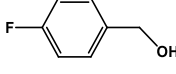
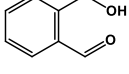
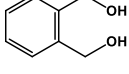
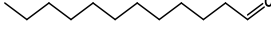
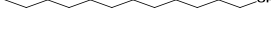
As is well known, homogeneous Lewis acids can effectively promote the CTH process, whereas the Brønsted acids

cannot catalyze this reaction. The mechanism for homogeneous CTH process is commonly accepted to involve a cyclic six-membered transition state in which both the reducing alcohol and the carbonyl compound are coordinated to the same Lewis acidic center [37, 56]. In a heterogeneous system, the surface Lewis acidic sites [37, 48], Brønsted acidic sites [52, 57, 58] and Basic sites [39, 50] were all found to be active for CTH reaction. Base on the nature of Al_2O_3 (abundant Lewis acidic sites) and previous studies on CTH reaction [26, 30, 37, 49, 51], we proposed a possible reaction mechanism. As shown in Scheme 3, 2-propanol was first activated and adsorbed on the surface Lewis acidic sites (Al^{3+}) of Al_2O_3 to form the corresponding alkoxide (step I), followed by activation and adsorption of the C=O bond of FUR on the same Lewis acidic sites (step II). Subsequently, a six-membered ring transition state was formed between FUR and 2-propanol by the hydrogen transfer process (step III). Finally, ring-opening occurred (step IV) and the FAL was desorbed from Al_2O_3 along with acetone (step V) to complete the catalytic cycle.

4 Conclusions

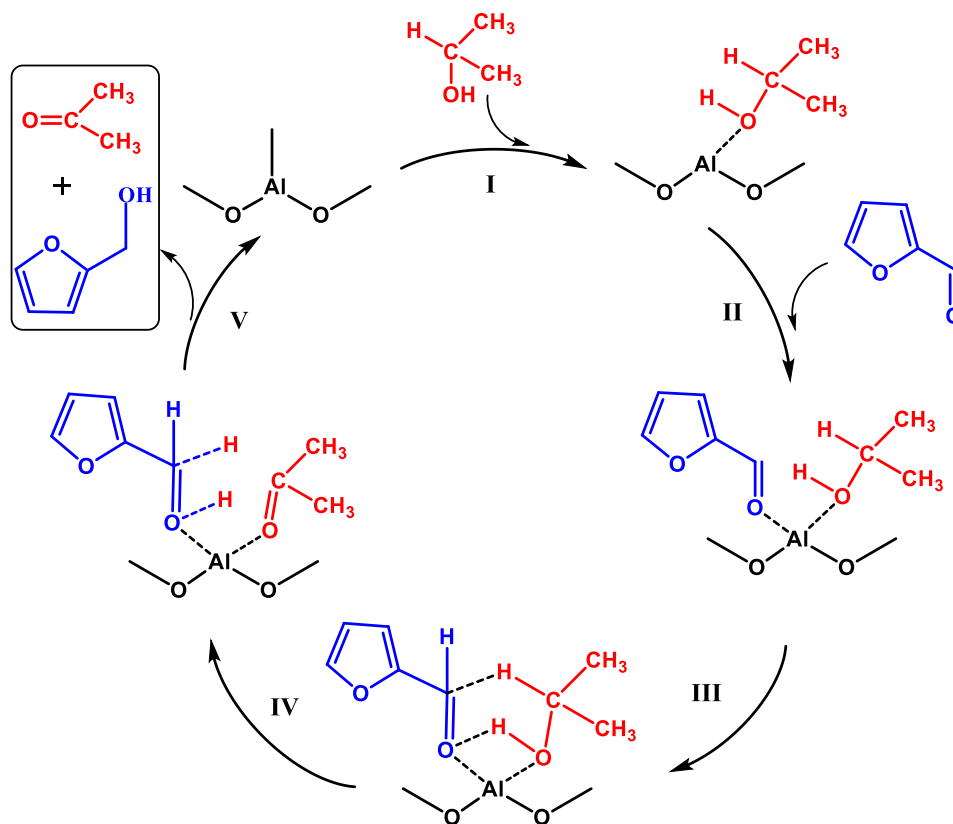
In summary, a series of single metal oxides with different acid–base nature include Al_2O_3 , MgO , ZrO_2 and Fe_2O_3 catalysts were prepared by precipitation method and then used to catalyze the CTH of FUR to FAL reaction. It is found that the as-prepared Al_2O_3 catalyst is identified as the most effective for FAL production, giving a FUR conversion as high as 96.5% and FAL selectivity of 99% after 1 h at 150 °C using 2-propanol as the H-donor and solvent. The Al_2O_3 has a large specific surface area and high density of surface

Table 5 Catalytic performance of Al_2O_3 catalyst for other aldehydes^a

Entry	Substrate	Product	Temp. (°C)	Time (h)	Conv. (%)	Sel. (%)
1			150	1	66	99
2			150	1	36	75
3			150	4	71	88
4			150	4	45	83
5			150	4	58	72
6			150	4	52	82

^aReaction conditions: 2 mmol Substrate, 10 mL 2-propanol, 50 mg Al_2O_3 , 0.8 MPa N_2

Scheme 3 Possible reaction mechanism for the CTH of FUR to FAL over Al_2O_3 catalyst



acidic, which were beneficial to FAL production from FUR. The catalytic data also showed that reaction time, reaction temperature and catalyst dosage have little effect on FAL selectivity (> 95%) but had a big influence on catalyst activity. Compared to other alcohols, 2-propanol was the most effective H-donor for the CTH reaction of FUR to FAL. The Arrhenius plots showed an E_a value of 15.2 kJ/mol, which is much lower than other catalysts. The prepared Al_2O_3 also showed a good catalytic performance for the others aldehydes and has a good application in industry.

Acknowledgements This work was supported by National Natural Science Foundation of China (21878027), Advanced Catalysis and Green Manufacturing Collaborative Innovation Center (ACGM2020-08), Natural Science Foundation of the Jiangsu Higher Education Institutions (18KJA150001) and the Open Fund of the Key Lab of Organic Optoelectronics & Molecular Engineering.

Declarations

Conflict of interest There are no conflicts to declare.

References

- Li JQ (2001) *Chem Eng J* 81:338–339
- Li X, Jia P, Wang T (2016) *ACS Catal* 6:7621–7640
- Mariscal R, Maireles-Torres P, Ojeda M, Sadaba I, Lopez Granados M (2016) *Energy Environ Sci* 9:1144–1189
- Villaverde MM, Bertero NM, Garetto TF, Marchi AJ (2013) *Catal Today* 213:87–92
- Gong W, Chen C, Zhang H, Zhang Y, Zhang Y, Wang G, Zhao H (2017) *Mol Catal* 429:51–59
- Song S, Guo H, Yin G (2011) *Catal Commun* 12:731–733
- Guo H, Yin G (2011) *J Phys Chem C* 115:17516–17522
- Li X, Ho B, Zhang Y (2016) *Green Chem* 18:2976–2980
- Tong X, Liu Z, Yu L, Li Y (2015) *Chem Commun* 51:3674–3677
- Tong X, Liu Z, Hu J, Liao S (2016) *Appl Catal A* 510:196–203
- Liu Z, Tong X, Liu J, Xue S (2016) *Catal Sci Technol* 6:1214–1221
- Wan W, Jenness GR, Xiong K, Vlachos DG, Chen JG (2017) *ChemCatChem* 9:1701–1707
- Manzoli M, Menegazzo F, Signoretto M, Cruciani G, Pinna F (2015) *J Catal* 330:465–473
- Signoretto M, Menegazzo F, Contessotto L, Pinna F, Manzoli M, Boccuzzi F (2013) *Appl Catal B* 129:287–293
- Cai CM, Zhang T, Kumar R, Wyman CE (2014) *J Chem Technol Biotechnol* 89:2–10
- Adkins H (2004) *Org React* 8:1–27
- Yu W, Tang Y, Mo L, Ping C, Hui L, Zheng X (2011) *Bioresour Technol* 102:8241–8246
- Merlo AB, Vetere V, Ruggera JF, Casella ML (2009) *Catal Commun* 10:1665–1669
- Johnstone RA, Wilby AH, Entwistle ID (1985) *Chem Rev* 85:129–170
- Neeli CKP, Chung Y-M, Ahn W-S (2017) *ChemCatChem* 9:4570–4579

21. García-Sancho C, Jiménez-Gómez CP, Viar-Antuñano N, Cecilia JA, Moreno-Tost R, Mérida-Robles JM, Requies J, Maireles-Torres P (2021) *Appl Catal A* 609:117905–117918
22. Scholz D, Aellig C, Hermans I (2014) *Chemsuschem* 7:268–275
23. Reddy Kannapu HP, Mullen CA, Elkasabi Y, Boateng AA (2015) *Fuel Process Technol* 137:220–228
24. Li J, Liu JL, Zhou HJ, Fu Y (2016) *Chemsuschem* 9:1339–1347
25. Li H, He J, Riisager A, Saravanamurugan S, Song B, Yang S (2016) *ACS Catal* 6:7722–7727
26. He J, Schill L, Yang S, Riisager A (2018) *ACS Sustain Chem Eng* 6:17220–17229
27. He J, Li H, Riisager A, Yang S (2018) *ChemCatChem* 10:430–438
28. Chen H, Ruan H, Lu X, Fu J, Langrish T, Lu X (2018) *Mol Catal* 445:94–101
29. Xiao P, Zhu J, Zhao D, Zhao Z, Zaera F, Zhu Y (2019) *ACS Appl Mater Interfaces* 11:15517–15527
30. Xu G, Liu C, Hu A, Xia Y, Wang H, Liu X (2019) *Mol Catal* 475:110384
31. Ma M, Hou P, Cao J, Liu H, Yan X, Xu X, Yue H, Tian G, Feng S (2019) *Green Chem* 21:5969–5979
32. Ma M, Hou P, Zhang P, Cao J, Liu H, Yue H, Tian G, Feng S (2020) *Appl Catal A* 602:117709–117718
33. Kumar A, Srivastava R (2020) *ACS Sustain Chem Eng* 8:9497–9506
34. Ramos R, Peixoto AF, Arias-Serrano BI, Soares OSGP, Pereira MFR, Kubička D, Freire C (2020) *ChemCatChem* 12:1467–1475
35. Li F, Jiang S, Huang J, Wang Y, Lu S, Li C (2020) *New J Chem* 44:478–486
36. Qiu M, Guo T, Xi R, Li D, Qi X (2020) *Appl Catal A* 602:117719–117725
37. Gao Z-K, Hong Y-C, Hu Z, Xu B-Q (2017) *Catal Sci Technol* 7:4511–4519
38. Wang H, Liu B, Liu F, Wang Y, Lan X, Wang S, Ali B, Wang T (2020) *ACS Sustain Chem Eng* 8:8195–8205
39. Wang F, Ta N, Shen W (2014) *Appl Catal, A* 475:76–81
40. Mei C, Dumesic JA (2011) *Chem Commun* 47:12233–12235
41. Tang X, Hu L, Sun Y, Zhao G, Hao W, Lin L (2013) *RSC Adv* 3:10277–10284
42. Komanoya T, Nakajima K, Kitano M, Hara M (2015) *J Phys Chem C* 119:26540–26546
43. Heidari H, Abedini M, Nemati A, Amini MM (2009) *Catal Lett* 130:266–270
44. Aramendía MA, Borau V, Jiménez C, Marinas JM, Ruiz JR, Urbano FJ (2003) *Appl Catal A* 244:207–215.
45. Miñambres JF, Aramendía MA, Marinas A, Marinas JM, Urbano FJ (2011) *J Mol Catal A: Chem* 338:121–129
46. Vingurt D, Fuks D, Landau MV, Vidruk R, Herskowitz M (2013) *Phys Chem Chem Phys* 15:14783–14796
47. Yu Z, Lu X, Wang X, Xiong J, Li X, Zhang R, Ji N (2020) *Chemsuschem* 13:5185–5198
48. Gilkey MJ, Panagiotopoulou P, Mironenko AV, Jenness GR, Vlachos DG, Xu B (2015) *ACS Catal* 5:3988–3994
49. Zhang J, Liu Y, Yang S, Wei J, He L, Peng L, Tang X, Ni Y (2020) *ACS Sustain Chem Eng* 8:5584–5594
50. Gliński M, Czajka A, Ulkowska U (2015) *React Kinet Mech Catal* 114:279–294
51. López-Asensio R, Cecilia JA, Jiménez-Gómez CP, García-Sancho C, Moreno-Tost R, Maireles-Torres P (2018) *Appl Catal A* 556:1–9
52. Li F, France LJ, Cai Z, Li Y, Liu S, Lou H, Long J, Li X (2017) *Appl Catal B* 214:67–77
53. Jiang S, Li F, Huang J, Wang Y, Lu S, Li P, Li C (2020) *ChemistrySelect* 5:9883–9892
54. Vasanthakumar P, Sindhuja D, Senthil Raja D, Lin C-H, Karvembu R (2020) *New J Chem* 44:8223–8231
55. Xiao P, Xuelian X, Wang S, Zhu J, Zhu Y (2020) *Appl Catal A* 603:117742–117749
56. Ponndorf W (1926) *Angew Chem* 39:138–143
57. Tang X, Chen H, Hu L, Hao W, Sun Y, Zeng X, Lin L, Liu S (2014) *Appl Catal B* 147:827–834
58. Zhu Y, Liu S, Jaenicke S, Chuah G (2004) *Catal Today* 97:249–255

Publisher's Note Springer Nature remains neutral with regard to jurisdictional claims in published maps and institutional affiliations.

Authors and Affiliations

Zonghui Liu¹  · Zhongze Zhang¹ · Zhe Wen¹ · Bing Xue¹

✉ Zonghui Liu
liuzh@cczu.edu.cn

✉ Bing Xue
xuebing@cczu.edu.cn

¹ Jiangsu Key Laboratory of Advanced Catalytic Materials and Technology, School of Petrochemical Engineering, Changzhou University, Changzhou 213164, Jiangsu, China